

UNBIASED SURVEYS OF DUST-ENSHROUDED GALAXIES USING ALMA

K. Kohno¹, S. Fujimoto^{2,3}, A. Tsujita¹, V. Kokorev⁴, G. Brammer^{3,5}, G. E. Magdis^{3,5},
 F. Valentino^{3,6}, N. Laporte^{7,8}, Fengwu Sun⁹, E. Egami⁹, F. E. Bauer¹⁰, A. Guerrero¹¹,
 N. Nagar¹¹, K. I. Caputi⁴, G. B. Caminha¹², J.-B. Jolly¹³, K. K. Knudsen¹⁴, R. Uematsu¹⁵,
 Y. Ueda¹⁵, M. Oguri¹⁶, A. Zitrin¹⁷, M. Ouchi^{18,19}, Y. Ono¹⁹, J. González-López^{20,21},
 J. Richard²², I. Smail²³, D. Coe²⁴, M. Postman²⁴, L. Bradley²⁴, A. M. Koekemoer²⁴,
 A. M. Muñoz Arancibia²⁵, M. Dessauges-Zavadsky²⁶, D. Espada²⁷, H. Umehata²⁸, B. Hatsukade¹,
 F. Egusa¹, K. Shimasaku²⁹, K. Matsui-Morokuma³⁰, W.-H. Wang³¹, T. Wang³², Y. Ao³³,
 A. J. Baker³⁴, Minju M. Lee³, C. del P. Lagos³⁵, D. H. Hughes³⁶ and ALCS collaboration

¹ Institute of Astronomy, Graduate School of Science, The University of Tokyo, 2-21-1 Osawa, Mitaka, Tokyo,
 e-mail: kkohno@ioa.s.u-tokyo.ac.jp

² Department of Astronomy, The University of Texas at Austin

³ Cosmic Dawn Center (DAWN)

⁴ Kapteyn Astronomical Institute, University of Groningen

⁵ Niels Bohr Institute, University of Copenhagen

⁶ European Southern Observatory

⁷ Kavli Institute for Cosmology, University of Cambridge

⁸ Cavendish Laboratory, University of Cambridge

⁹ Steward Observatory, University of Arizona

¹⁰ Instituto de Astrofísica, Facultad de Física, Pontificia Universidad Católica de Chile

¹¹ Departamento de Astronomía, Universidad de Concepción

¹² Max-Planck-Institut für Astrophysik

¹³ Max-Planck-Institut für extraterrestrische Physik

¹⁴ Department of Space, Earth and Environment, Chalmers University of Technology, Onsala Space Observatory

¹⁵ Department of Astronomy, Kyoto University

¹⁶ Center for Frontier Science, Chiba University

¹⁷ Physics Department, Ben-Gurion, University of the Negev

¹⁸ National Astronomical Observatory of Japan

¹⁹ Institute for Cosmic Ray Research, The University of Tokyo

²⁰ Núcleo de Astronomía de la Facultad de Ingeniería y Ciencias, Universidad Diego Portales

²¹ Las Campanas Observatory, Carnegie Institution of Washington

²² Univ Lyon, Univ Lyon1, Ens de Lyon, CNRS, Centre de Recherche Astrophysique de Lyon

²³ Centre for Extragalactic Astronomy, Department of Physics, Durham University

²⁴ Space Telescope Science Institute

²⁵ Millennium Institute of Astrophysics (MAS); Center for Mathematical Modeling (CMM), Universidad de Chile

²⁶ Observatoire de Genève, Université de Genève

²⁷ Departamento de Física Teórica y del Cosmos, Campus de Fuentenueva, Edificio Mecenas, Universidad de Granada

²⁸ Institute for Advanced Research, Nagoya University

²⁹ Department of Astronomy, Graduate School of Science, The University of Tokyo

³⁰ University of Tsukuba

³¹ Institute of Astronomy and Astrophysics, Academia Sinica

³² Key Laboratory of Modern Astronomy and Astrophysics, Nanjing University

³³ Purple Mountain Observatory and Key Laboratory for Radio Astronomy, Chinese Academy of Sciences

³⁴ Department of Physics and Astronomy, Rutgers, the State University of New Jersey

³⁵ International Centre for Radio Astronomy Research (ICRAR), M468, University of Western Australia

³⁶ Instituto Nacional de Astrofísica, Óptica y Electrónica (INAOE)

Abstract. The ALMA lensing cluster survey (ALCS) is a 96-hr large program dedicated to uncovering and characterizing intrinsically faint continuum sources and line emitters with the assistance of gravitational lensing. All 33 cluster fields were selected from *HST/Spitzer* treasury programs including CLASH, Hubble Frontier Fields, and RELICS, which also have *Herschel* and *Chandra* coverages. The total sky area surveyed reaches ~ 133 arcmin 2 down to a depth of $\sim 60 \mu\text{Jy beam}^{-1}$ (1σ) at 1.2 mm, yielding 141 secure blind detections of continuum sources and additional 39 sources aided by priors. We present scientific motivation, survey design, the status of spectroscopy follow-up observations, and number counts down to $\sim 7 \mu\text{Jy}$. Synergies with *JWST* are also discussed.

1 Introduction

Long after the pioneering submillimeter (submm) surveys of lensing clusters using SCUBA (e.g., Smail et al. 1997; Knudsen et al. 2008), the advent of ALMA has enabled us to uncover faint ($S_{1.2\text{mm}} \lesssim 1 \text{ mJy}$) (sub)mm-selected galaxies, which are significantly (up to $\sim 100\times$) fainter than “classical” submm galaxies (SMGs, $S_{870\mu\text{m}} \gtrsim \text{a few mJy}$), by individual pointed observations (e.g., Hatsukade et al. 2013; Fujimoto et al. 2016; Gruppioni et al. 2020) including ALMA calibrators (Chen et al. 2023) and unbiased deep surveys of a contiguous region like HUDF/GOODS-S (e.g., Aravena et al. 2016, 2020; Dunlop et al. 2017; Hatsukade et al. 2018; Franco et al. 2018; González-López et al. 2017, 2020). These faint submm sources are the major contributor to the cosmic infrared background (CIB) light (e.g., Fujimoto et al. 2016), in contrast to the classical bright SMGs. However, the resolved fraction of CIB remains controversial (e.g., Muñoz Arancibia et al. 2018). Furthermore, a fraction of faint ALMA sources are invisible even in the deepest NIR images using *HST* (e.g., Simpson et al. 2014; Fujimoto et al. 2016; González-López et al. 2017; Cowie et al. 2018; Schreiber et al. 2018; Franco et al. 2018; Yamaguchi et al. 2019; Casey et al. 2019; Williams et al. 2019; Umehata et al. 2020; Gruppioni et al. 2020; Manning et al. 2022; Shu et al. 2022). Recent studies point to the importance of *H*-band-dark but IRAC-detected (a.k.a. *H*-dropout) galaxies as a key tracer of the early phases of massive galaxy formation, which are not captured by the Lyman break technique relying on the rest-frame UV light (e.g., Caputi et al. 2014; Wang et al. 2019). Smail et al. (2021) revealed that SMGs tend to have compact dust continuum size, and more obscured sources tend to exhibit higher star formation rate surface density Σ_{SFR} , claiming that the extreme, optically dark SMGs are forming spheroids at high redshifts. Despite this importance, the difficulties to obtain accurate (i.e., spectroscopic) redshifts of these *H*-dropout faint ALMA galaxies (either optical/near-IR spectroscopy or mm/submm line scans) hamper the efforts to characterize them. These facts therefore strongly motivate us to search for gravitationally magnified (but intrinsically faint) *H*-dropout ALMA sources.

2 ALMA Lensing Cluster Survey

The base sample of clusters is defined as follows. (1) observed by *Planck*, i.e., SZE-based mass measurements are available, (2) $z > 0.1$, (3) observed by *HST/ACS* with three or more filters, (4) and at least two orbits WFC3/IR (equivalent to the depth of the HST treasury program CANDELS; Grogan et al. 2011; Koekemoer et al. 2011) with four or more filters, (5) also observed by *Spitzer/IRAC*, and (6) in the declination range suited for ALMA, i.e., $-75^\circ < \delta < +25^\circ$, to ensure shadowing of less than 5%. The samples are selected from the best-studied clusters drawn from Cluster Lensing And Supernova Survey with Hubble (CLASH; Postman et al. 2012), Hubble Frontier Fields (HFF; Lotz et al. 2017), and the Reionization Lensing Cluster Survey (RELICS; Coe et al. 2019). We find that 60 clusters fulfill the criteria, and for ALMA cycle-6 we select 33 clusters with the most accurate mass models determined so far, after excluding clusters in the ALMA archive. The total sky area surveyed reaches ~ 133 arcmin 2 down to a depth of $\sim 60 \mu\text{Jy beam}^{-1}$ (1σ) at 1.2 mm. Fig. 0.1 gives the survey area of ALCS, along with other ALMA surveys. It yields 141 secure blind detections of continuum sources and additional 39 sources aided by priors (Fujimoto et al. in prep.). Fig.0.2 presents an example of the ALCS fields, RXC J0032.1+1808. It shows rich ALMA 1.2 mm sources, including known multiply imaged dusty galaxy at $z = 3.631$ (Dessauges-Zavadsky et al. 2017, not visible in the Figure). Two sets of triple-image *H*-dropout sources have been uncovered (Sun et al. 2022, Tsujita et al., in prep.). An association of a highly magnified ($\mu \sim 10$) *H*-dropout ALMA source with a MUSE-selected galaxy group at $z = 4.32$ behind “El Gordo” cluster suggests that such dust-enshrouded ALMA sources can be signposts of richer star-forming environments at high redshifts (Caputi et al. 2021). Multi-wavelength mosaics across all 33 ALCS fields and photometric catalogs by reprocessing archival data

from *Hubble* & *Spitzer* have been created (Kokorev et al. 2022). This rich source catalog has been used to conduct stacking analysis (e.g., Jolly et al. 2021). Joint analysis with *Herschel* has been conducted to investigate far-infrared SEDs of ALCS sources (Sun et al. 2022). A spin-out program to search for lensed *H*-dropout/faint IRAC sources has been launched (Sun et al. 2021). *Chandra* X-ray properties of ALCS sources have been investigated (Uematsu et al. 2023).

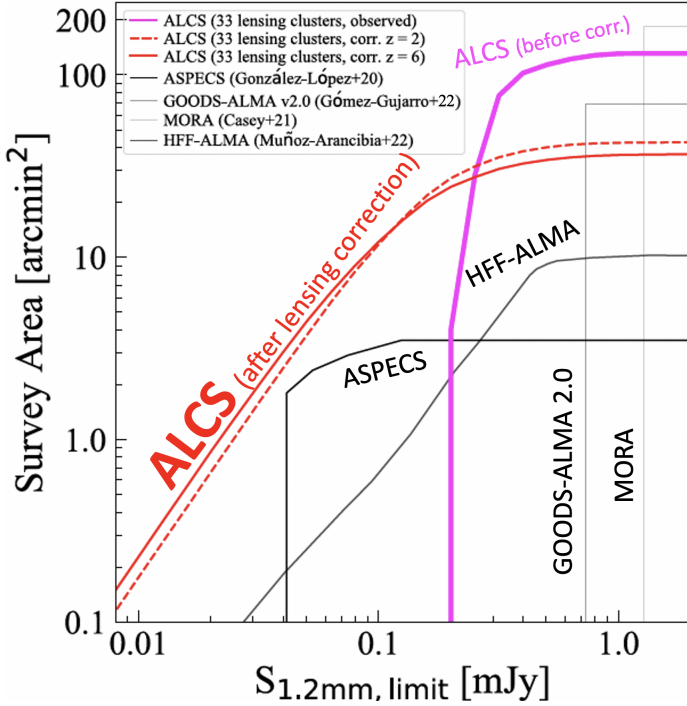


Figure 0.1. Survey areas of ALCS ($\text{SNR} > 4.0$, the primary beam response of $\gtrsim 30\%$) and other large ALMA surveys in the literature (González-López et al. 2020; Gómez-Guijarro et al. 2022; Casey et al. 2021; Muñoz Arancibia et al. 2022). The magenta line denotes the survey area before the lensing correction. The red dashed and solid lines represent the effective survey area after the lensing correction, assuming the redshift at $z = 2.0$ and $z = 6.0$, respectively, with our fiducial lens models. ALCS explores the unique parameter space towards faint and wide regimes, compared to previous ALMA surveys, by exploiting a natural telescope in space, i.e., cluster lensing.

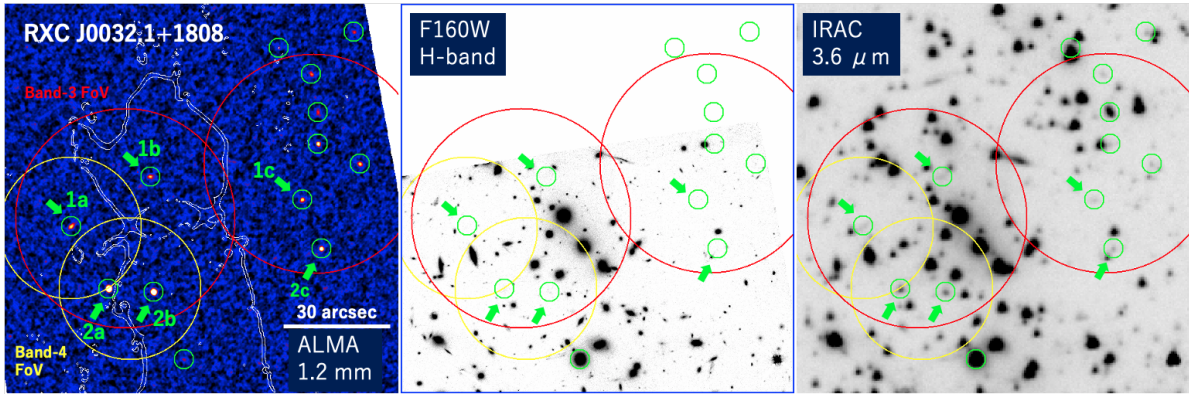


Figure 0.2. ALCS 1.2 mm continuum (left), *HST*/WFC3 *H*-band (middle), and *Spitzer*/IRAC 3.6 μm images of RXC J0032.1+1808. Two sets of triple image *H*-dropout sources (1a/1b/1c and 2a/2b/2c) are identified. The analysis of ALMA Band-3/4 spectral scans (red and yellow circles) will be presented elsewhere (Tsujita et al., in prep.).

Multiple ALMA follow-up programs to conduct spectral scans toward *H*- and IRAC-dropout ALCS 1.2 mm sources have been conducted. Figure 0.3 shows a triple image *H*-dropout ALMA source behind MACS J0417.5-1154 and its band-3/4 spectra, giving $z_{\text{CO}} = 3.652$ (Tsujita et al., in prep.).

3 Number Counts

Figure 0.4 shows the differential number counts constructed by the ALCS 1.2 mm continuum source catalog. A detailed description of number counts and subsequent discussions will be given in a forthcoming paper (Fujimoto et al. 2023). With the blind sample, we derive 1.2-mm number counts down to $\sim 7 \mu\text{Jy}$ assisted by the gravitational lensing, and find that the total integrated 1.2 mm flux of the securely identified sources

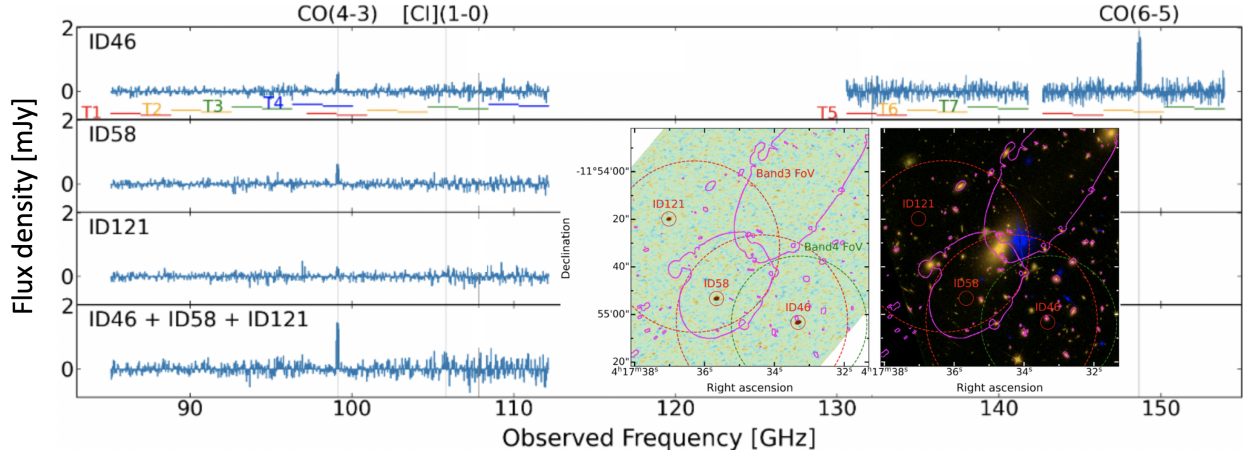


Figure 0.3. ALMA band-3/4 spectra for ALCS 1.2-mm continuum sources, ID46, ID58, and ID121, in MACS J0417.5-1154 produced by combining seven independent tunings (T1–T7). The inserted panels display the ALCS 1.2-mm continuum (left) and *HST* 3-color composite (right; RGB = F160W, F125W, F814W), along with the positions of three sources and the critical curve at $z = 3.7$ (magenta contours). The thin horizontal lines indicate the expected observed frequencies of the CO(4–3), [C I] (${}^3\text{P}_1 - {}^3\text{P}_0$), and CO(6–5) at the resultant spectroscopic redshift $z_{\text{CO}} = 3.652$, which is consistent with the predictions from the mass/lens model of this field.

corresponds to $\sim 80\%$ of the CIB light. We find a steady increase in the number counts even below $S_{1.2\text{mm}} < 0.1 - 0.01 \text{ mJy}$, which does not support the flattening shape argued in HUDF (González-López et al. 2020). It urges us to further investigate the faint-end of the 1-mm number counts by extending unbiased ALMA deep surveys and/or systematically increasing the spec- z sample in the lensing fields and ultimately improving the precision of the amplification estimates.

4 Synergies with JWST and future prospects

An exceptionally magnified ($\mu \sim 20 - 160$), intrinsically faint (sub- L^* -class) low-mass ($M_* \sim 10^9 M_\odot$) star-forming galaxy at $z = 6.07$ (Laporte et al. 2021; Fujimoto et al. 2021), which is one of the early outcomes of an unbiased line emitter search using the ALCS 3D cube, is scheduled to be observed by *JWST*/NIRCam, NIRSpec, VLT/MUSE, and so on. *JWST* observations of lensing clusters including ALCS fields are now rapidly increasing, allowing us to characterize ALCS 1.2 mm continuum sources in e.g., SMACS J0723.3-7327 (Cheng et al. 2022; Fudamoto et al. 2022) and Abell 2744 (Kokorev et al. 2023).

Recent *JWST*/NIRCam observations report a remarkably high abundance of NIR-dropout sources, i.e., “ultra-high-redshift” LBG candidates (e.g., Finkelstein et al. 2023; Bouwens et al. 2023; Donnan et al. 2023; Harikane et al. 2023), which may violate the current galaxy formation models based on the Λ -CDM framework (Naidu et al. 2022; Lovell et al. 2023). ALMA spectroscopy observations of an ultra-high- z candidate suggest that a part of such ultra-high- z candidates may be dust-enshrouded star-forming galaxies at $z \sim 4 - 5$ (Fujimoto et al. 2022), implying a potential overlap with the H -band dropout sources. Therefore, further investigation of the physical properties of H - and IRAC-dropout sources uncovered by ALCS will help the interpretation of the putative ultra-high-redshift candidates.

References

- Aravena, M.; Decarli, R.; Walter, F. et al. 2016, ApJ, 833, 68
- Aravena, M.; Boogaard, L.; Gómez-González, J. et al. 2020, ApJ, 901, 79
- Béthermin, M.; Fudamoto, Y.; Ginolfi, M. et al. 2020, A&A, 643, A2
- Bouwens, R., Illingworth, G., Oesch, P., et al. 2023, MNRAS, in press
- Carniani, S.; Maiolino, R.; De Zotti, G. et al. 2015, A&A, 584, A78
- Caputi, K. I.; Michałowski, M. J.; Krips, M. et al. 2014, ApJ, 788, 126
- Caputi, K. I.; Caminha, G. B.; Fujimoto, S. et al. 2021, ApJ, 908, 146
- Casey, C. M.; Zavala, J. A.; Aravena, M. et al. 2019, ApJ, 887, 55
- Casey, C. M.; Zavala, J. A.; Manning, S. M. et al. 2021, ApJ, 923, 215

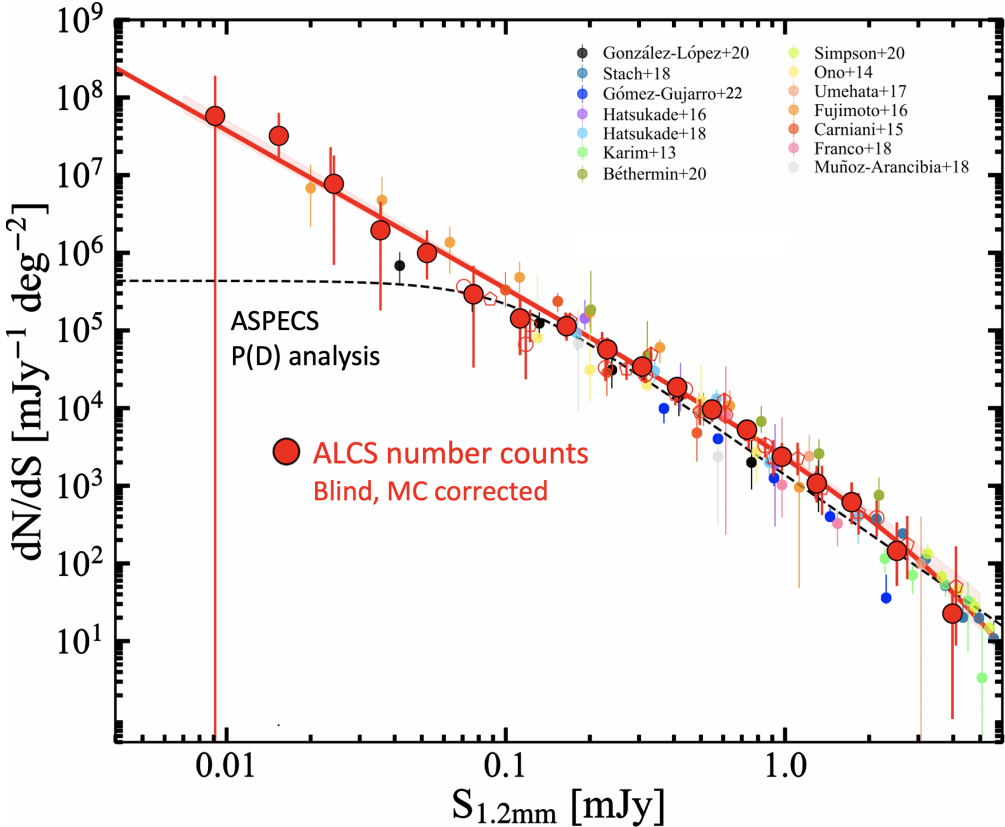


Figure 0.4. Differential number counts at 1.2 mm (Fujimoto et al. 2023). The filled red circles represent the ALCS number counts using the blindly identified sources corrected by the MC simulations that implement relevant uncertainties such as z , μ , and flux density measurements, where the error bars indicate the 16–84th percentile in the 5,000 MC realizations. The red line and the shaded region denote the best-fit Schechter function and the associated 1σ error. The faint-end flattening of the ASPECS number counts estimated by $P(D)$ analysis (González-López et al. 2020) is shown (dashed line). For measurements observed at different wavelengths from 1.2 mm, we scale the flux density by assuming a typical FIR SED shape based on a single modified black body with $T_{\text{dust}} = 35$ K, spectral index $\beta = 1.8$, and $z = 2$.

- Chen, J.; Ivison, R. J.; Zwaan, M. A. et al. 2023, MNRAS, 518, 1378
 Cheng, C.; Yan, H.; Huang, J.-S. et al. 2022, ApJL, 936, L19
 Coe, D.; Salmon, B.; Bradač, M. et al. 2019, ApJ, 884, 85
 Cowie, L. L.; González-López, J.; Barger, A. J. et al. 2018, ApJ, 865, 106
 Dessauges-Zavadsky, M.; Zamojski, M.; Rujopakarn, W. et al. 2017, A&A, 605, A81
 Donnan, C. T., McLeod, D. J., Dunlop, J. S., et al. 2023, MNRAS, 518, 6011
 Dunlop, J. S.; McLure, R. J.; Biggs, A. D., et al. 2017, MNRAS, 466, 861
 Finkelstein, S. L., Bagley, M. B., Ferguson, H. C., et al. 2023, ApJL, 946, L13
 Franco, M.; Elbaz, D.; Béthermin, M. et al. 2018, A&A, 620, A152
 Fudamoto, Y.; Inoue, A. K.; & Sugahara, Y. 2022, ApJL, 938, L24
 Fujimoto, S.; Ouchi, M.; Ono, Y. et al. 2016, ApJS, 222, 1
 Fujimoto, S.; Oguri, M.; Brammer, G. et al. 2021, ApJ, 911, 99
 Fujimoto, S.; Finkelstein, S. L.; Burgarella, D., et al. submitted to ApJ (arXiv:2211.03896)
 Fujimoto, S., Kohno, K., Ouchi, M., et al. submitted to ApJS (arXiv:2303.01658)
 Gómez-Guijarro, C.; Elbaz, D.; Xiao, M.; et al. 2022, A&A, 658, A43
 González-López, J.; Bauer, F. E.; Aravena, M. et al. 2017, A&A, 608, A138
 González-López, J.; Novak, M.; Decarli, R. et al. 2020, ApJ, 897, 91
 Grogin, N. A., Kocevski, D. D., Faber, S. M., et al. 2011, ApJS, 197, 35
 Gruppioni, C.; Béthermin, M.; Loiacono, F. et al. 2020, A&A, 643, A8

- Harikane, Y.; Ouchi, M., Oguri, M., et al. ApJS, in press (arXiv:2208.01612)
- Hatsukade, B.; Ohta, K.; Seko, A. et al. 2013, ApJL, 769, L27
- Hatsukade, B.; Kohno, K.; Umehata, H. et al. 2016, PASJ, 68, 36
- Hatsukade, B.; Kohno, K.; Yamaguchi, Y. et al. 2018, PASJ, 70, 105
- Jolly, J.-B.; Knudsen, K.; Laporte, N. et al. 2021, A&A, 652, A128
- Karim, A.; Swinbank, A. M.; Hodge, J. A. et al. 2013, MNRAS, 432, 2
- Koekemoer, A. M., Faber, S. M., Ferguson, H. C., et al. 2011, ApJS, 197, 36
- Kokorev, V.; Brammer, G.; Fujimoto, S. et al. 2022, ApJS, 263, 38
- Kokorev, V.; Jin, S.; Magdis, G. E. et al. submitted to ApJL (arXiv:2301.04158)
- Knudsen, K. K.; van der Werf, P. P.; & Kneib, J.-P. 2008, MNRAS, 384, 1611
- Lagos, C. del P.; da Cunha, E.; Robotham, A. S. G. et al. 2020, MNRAS, 499, 1948
- Laporte, N.; Zitrin, A.; Ellis, R. S. et al. 2021, MNRAS, 505, 4838
- Lotz, J. M.; Koekemoer, A.; Coe, D. et al. 2017, ApJ, 837, 97
- Lovell, C. C., Harrison, I., Harikane, Y., et al. 2023, MNRAS, 518, 2511
- Manning, S. M.; Casey, C. M.; Zavala, J. A. et al. 2022, ApJ, 925, 23
- Muñoz Arancibia, A. M.; González-López, J.; Ibar, E. et al. 2018, A&A, 620, A125
- Muñoz Arancibia, A. M.; González-López, J.; Ibar, E. et al. submitted to A&A (arXiv:2203.06195)
- Naidu, R. P., Oesch, P. A., Setton, D. J., et al. submitted to ApJL (arXiv:2208.02794)
- Ono, Y.; Ouchi, M.; Kurono, Y.; et al. 2014, ApJ, 795, 5
- Postman, M.; Coe, D.; Benítez, N. et al. 2012, ApJS, 199, 25
- Schreiber, C.; Labb  , I.; Glazebrook, K. et al. 2018, A&A, 611, A22
- Shu, X.; Yang, L.; Liu, D. et al. 2022, ApJ, 926, 155
- Simpson, J. M.; Swinbank, A. M.; Smail, I. et al. 2014, ApJ, 788, 125
- Simpson, J. M.; Smail, I.; Dudzevi  t  , U. et al. 2020, MNRAS, 495, 3409
- Smail, I.; Ivison, R. J.; & Blain, A. W. 1997, ApJL, 490, L5
- Smail, I.; Dudzevi  t  , U.; Stach, S. M. et al. 2021, MNRAS, 502, 3426
- Stach, S. M.; Smail, I.; Swinbank, A. M. et al. 2018, ApJ, 860, 161
- Sun, F.; Egami, E.; Fujimoto, S.; et al. 2022, ApJ, 932, 77
- Sun, F.; Egami, E.; P  rez-Gonz  lez, P. G. et al. 2021, ApJ, 922, 114
- Uematsu, R.; Ueda, Y.; Kohno, K. et al. ApJ, in press (arXiv:2301.09275)
- Umehata, H.; Tamura, Y.; Kohno, K. et al. 2017, ApJ, 835, 98
- Umehata, H.; Smail, I.; Swinbank, A. M. et al. 2020, A&A, 640, L8
- Wang, T.; Schreiber, C.; Elbaz, D. et al. 2019, Nature, 572, 211
- Williams, C. C.; Labbe, I.; Spilker, J. et al. 2019, ApJ, 884, 154
- Yamaguchi, Y.; Kohno, K.; Hatsukade, B. et al. 2019, ApJ, 878, 73